



## Regular Article

## In-situ neutron diffraction during stress relaxation of a single crystal nickel-base superalloy

David M. Collins<sup>a</sup>, Neil D'Souza<sup>b</sup>, Chinnapat Panwisawas<sup>c</sup><sup>a</sup>Department of Materials, University of Oxford, Parks Road, Oxford OX1 3PH, UK<sup>b</sup>Rolls-Royce plc, PO. Box 31, Derby DE24 8BJ, UK<sup>c</sup>School of Metallurgy and Materials, University of Birmingham, Edgbaston, Birmingham B15 2TT, UK

## ARTICLE INFO

## Article history:

Received 24 October 2016

Received in revised form 24 December 2016

Accepted 3 January 2017

Available online 26 January 2017

## Keywords:

Superalloys  
Neutron diffraction  
Single crystal  
Stress relaxation  
Lattice strain

## ABSTRACT

The stress relaxation behaviour of a single crystal nickel-base superalloy has been quantified using time-of-flight neutron diffraction analysis for a range of temperatures relevant to casting. A new iterative analysis methodology is described to isolate the lattice strain behaviour of the  $\gamma$  matrix and  $\gamma'$  precipitate phases from data obtained sufficiently rapidly to help elucidate the microscopic effect of macroscopic stress relaxation. The independent response of  $\gamma$  and  $\gamma'$  is revealed, showing the temperature sensitivity of lattice strain relaxation. The  $\gamma/\gamma'$  response is discussed in the context of thermo-mechanical conditions that may affect the propensity for recrystallisation.

© 2017 Acta Materialia Inc. Published by Elsevier Ltd. This is an open access article under the CC BY license (<http://creativecommons.org/licenses/by/4.0/>).

Nickel-base superalloys are typically chosen for turbine blade applications due their excellent high temperature mechanical and environmental properties. To confer suitable creep performance, the material is cast into a single crystal via directional solidification, involving a controlled mould withdrawal from the furnace. During this process, macroscopic residual stresses are produced in the component due to localised plastic flow induced from the different thermal expansions of the metal and the ceramic mould during cooling. These are sufficient for the metal to experience visco-plasticity through creep and stress relaxation, affecting the resultant dislocation density. This has implications to recrystallisation during subsequent processing heat treatments. Such artifacts are unacceptable during turbine blade manufacture. It is therefore critical to quantify macromechanical and micromechanical strains, in addition to their sensitivity to processing conditions.

An attractive method for quantifying micromechanical strains in nickel-base superalloys is diffraction via the evaluation of lattice strains. In particular, techniques that offer high angular resolution to separate the disordered A1  $\gamma$  matrix and ordered L1<sub>2</sub> structured  $\gamma'$  precipitates are desirable. Experiments are often complicated by the desire to obtain information at service or processing relevant stresses and/or temperatures. Laboratory X-ray sources can be equipped with in-situ testing capability, though their low flux and energy typically prohibits the measurement of the inherently weak  $\gamma'$  superlattice reflections. Experiments are instead commonly performed at either

synchrotron or neutron sources. To date, experimenters have investigated dynamic behaviour such as tensile [1,2], creep [3–5], processing heat treatments & phase transformations [6–9] and stress relaxation [10,11]. In this study, an analysis methodology is developed that enables quantification of  $\gamma$  and  $\gamma'$  lattice strains to investigate the stress relaxation behaviour in-situ during time-of-flight neutron diffraction measurements of a single crystal nickel-base superalloy. With a necessarily rapid data acquisition time to describe such phenomena, the new method enables analysis of diffraction data with a low signal to noise ratio that would be impossible using existing data fitting strategies.

As-cast cylindrical single crystal specimens of CMSX-4 nickel-base superalloy (Ni–5.6Al–9.0Co–6.5Cr–0.6Mo–3.0Re–6.5Ta–6.0W–0.1Hf, wt.%) were studied. Each specimen had a 5.85 mm diameter and 29 mm gauge length. They were processed and machined using conditions described in [11,12].

Time-of-flight diffraction experiments were performed on the ENGIN-X neutron diffractometer [13], ISIS, UK. The experimental setup adopted during the acquisition of neutron diffraction data is shown in Fig. 1. The neutron signal was obtained from a probed volume measuring  $8 \times 4 \times 4 \text{ mm}^3$ , controlled by the incident beam cross section and the collimator size. Samples were heated in an optical furnace at  $10 \text{ }^\circ\text{C min}^{-1}$  to  $800 \text{ }^\circ\text{C}$  then at  $5 \text{ }^\circ\text{C min}^{-1}$  to the test temperatures  $900 \text{ }^\circ\text{C}$ ,  $940 \text{ }^\circ\text{C}$ ,  $980 \text{ }^\circ\text{C}$  and  $1000 \text{ }^\circ\text{C}$  measured with a K-type thermocouple, followed by a 20 min hold period before

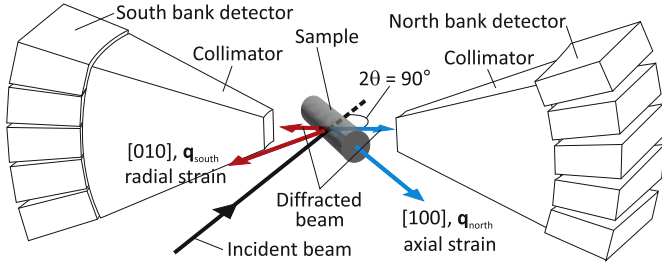


Fig. 1. Schematic illustration of the experimental setup on the ENGIN-X instrument at ISIS, Didcot, UK.

loading. Using a tensile rig on the beam line, four specimens were loaded at a strain rate of  $3.3 \times 10^{-5} \text{ s}^{-1}$  to different initial stress levels (600 MPa, 480 MPa, 400 MPa and 380 MPa). Stresses were held at these magnitudes under load control for 9 min. Thereafter, relaxation was conducted under displacement control for 9 min. The load, hold and relaxation cycle was repeated for 6–7 cycles, with each cycle increasing the macroscopic stress by 10 MPa.

The measurement of  $\gamma$  and  $\gamma'$  lattice parameters has been achieved by adopting a new data fitting strategy, developed from a previous methodology used for the analysis of X-ray diffraction data from polycrystalline nickel-base superalloys [9]. This method is tailored for time-of-flight neutron diffraction data from single crystal superalloys, incorporating the characteristic line profile asymmetry arising from the thermalisation process of neutrons, producing a time distribution of the neutron pulse [14]. The line profile shape used is a convolution product of a Voigt function and a trailing exponential function, where the former is defined as

$$V(x) = G(x) \otimes L(x) \quad (1)$$

where  $V(x)$  is the Voigt function,  $G(x)$  is the Gaussian function,  $L(x)$  is the Lorentzian function. The independent variable is  $x = d - d_c$  where  $d$  is d-spacing converted from time-of-flight and  $d_c$  is the d-spacing coordinate of the peak centre of mass. The full fitting function,  $V_{\text{exp}}(x)$ , is given by

$$V_{\text{exp}}(x) = V(x) \otimes \exp(-\eta|x|)H(x) \quad (2)$$

where  $\eta$  is a constant and  $H(x)$  is the Heaviside step function. The line profile asymmetry from the ENGIN-X instrument was determined by performing single peak fitting (using  $V_{\text{exp}}$  function) of a  $\text{CeO}_2$  standard on all reflections in the d-spacing range  $1.19 \text{ \AA} < d < 2.88 \text{ \AA}$ .

To correctly fit the superalloy diffraction patterns, the parameters contributing to the intensity of individual reflections are considered. Following [15], the integrated intensity,  $I$  of a polychromatic incident neutron beam for a single Laue spot is

$$I \propto \frac{I_0(\lambda_0)\lambda_0^4|F_{hkl}|^2 \Delta v}{2\sin^2\theta_0 v_a^2} \quad (3)$$

where  $I_0(\lambda_0)$  is the intensity-wavelength ( $\lambda_0$ ) distribution,  $F_{hkl}$  is the structure factor for reflection  $hkl$ ,  $\Delta v$  is the diffracted volume,  $v_a$  is the unit cell volume and  $\theta_0$  is the Bragg angle. For the fundamental  $\{200\}$  reflections (example (200) reflection shown in Fig. 2b), the measured intensity is the superposition of intensity from the  $\gamma$  ( $I_{200}^\gamma$ ) and  $\gamma'$  ( $I_{200}^{\gamma'}$ ) phases. As the  $\gamma/\gamma'$  lattice misfit for CMSX-4 is

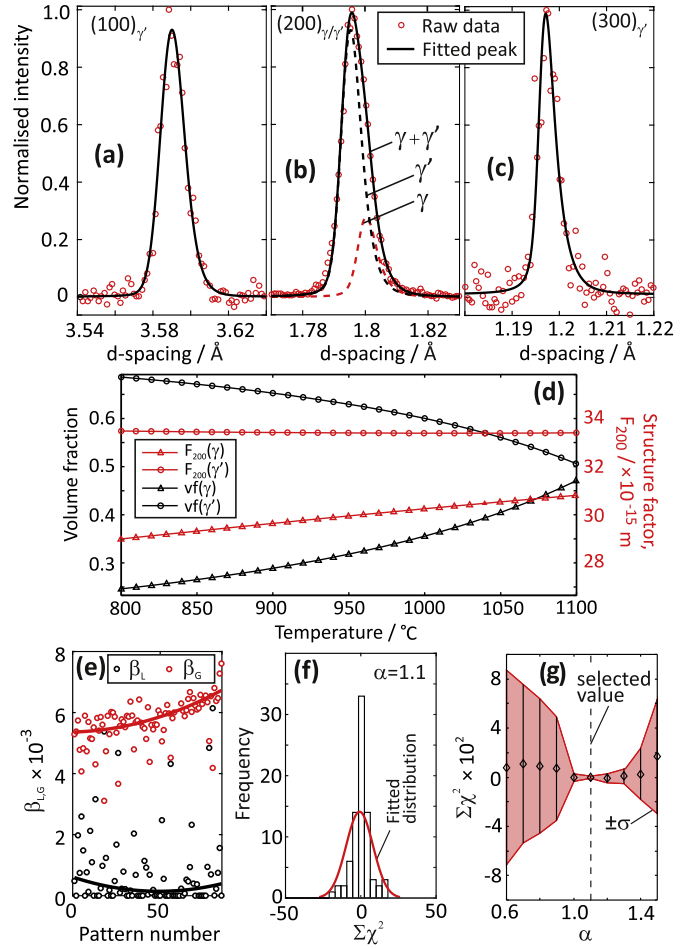


Fig. 2. Example diffraction reflections collected at 20 °C with no stress applied for (a) the superlattice (100) (b), fundamental (200), (c) superlattice (300), (d) predictions of  $\gamma$  &  $\gamma'$  volume fractions and calculated  $\{200\}$   $\gamma$  &  $\gamma'$  structure factors, (e) fitted  $\{200\}$   $\gamma$  Lorentzian breadth ( $\beta_L$ ) and Gaussian breadth ( $\beta_G$ ), (f) fitted distribution of  $\Sigma\chi^2$  errors for all patterns obtained from a sample, and (g) the effect of  $\alpha$  on  $\Sigma\chi^2$ .

small, (typically  $-5 \times 10^{-3}$  to  $1 \times 10^{-3}$  [16,17]) Eq. (3) can be used to express the ratio of intensity between the two reflections:

$$\frac{I_{200}^\gamma}{I_{200}^{\gamma'}} = \frac{|F_{200}^\gamma|^2 \Delta v^\gamma}{|F_{200}^{\gamma'}|^2 \Delta v^{\gamma'}} \quad (4)$$

All absent terms from Eq. (3) are eliminated, being equivalent for  $\gamma$  and  $\gamma'$  (including unit cell volumes where  $v_a^\gamma \approx v_a^{\gamma'}$ ). Whilst the above intensity expression has been simplified; neglecting absorption, extinction and thermal vibration effects is valid as their contributions are approximately cancelled in Eq. (3). For the  $\{200\}$   $\gamma$  reflection, the structure factor (simplified from general expressions, described elsewhere [9]) is

$$F_{200}^\gamma = 4 \sum c_Z b_Z \quad (5)$$

where  $c_Z$  is the composition and  $b_Z$  is the bound coherent scattering length for each element,  $Z$ , with terms for the latter tabulated in [18]. For the ordered  $L1_2$  structured  $\gamma'$  with a  $\text{Ni}_3\text{Al}$  stoichiometry, the  $\{200\}$  fundamental reflection structure factor is

$$F_{200}^{\gamma'} = 3 \sum_A c_{Z_A} b_{Z_A} + \sum_B c_{Z_B} b_{Z_B} \quad (6)$$

Download English Version:

<https://daneshyari.com/en/article/5443405>

Download Persian Version:

<https://daneshyari.com/article/5443405>

[Daneshyari.com](https://daneshyari.com)